A High Performance LiFePO₄ Cathode Material with 3D Conduction Network Connected by 1D helix-like Ag Nano-chains

Le Wen, Jiawei Liu,Jingjing Hou, Shuning Zhao, Jinli Liu, Zihao Zheng, Fengli Bei[*]

China National Quality Supervision and Inspection Center fou Industrial Explosive Materials, Nanjing University of Science and Technology, Nanjing, 210094, P.R. China.
[*]E-mail: beifl@njust.edu.cn

In this article, the original LiFePO₄/(C+RGO) cathode material with a uniform distribution of cuboid morphology was synthesized by hydrothermal method, and then 3 wt% nano silver was coated on the surface of the original material by a simple chemical deposition method. The surface structure and electrochemical performance of the original and modified cathode materials were characterized by XRD, SEM, TEM, and constant current charge/discharge tests. The results showed that the one-dimensional silver nano-chains with spiral structure and the two-dimensional graphene plane structure formed an uniform three-dimensional network coating layer , and the structure of the original material has not been changed. The cathode electrode material after coating had the best cycle and rate performance. The modified material had an initial charge-discharge capacity of 150.7 mAh·g^{-1} at 0.2C, which is 25.4% higher than the original material (LiFePO₄/C). Secondly, the cycle performance is improved. After the coated material was cycled at 0.2C for 100 cycles, the discharge capacity is 157mAh/g, and the capacity retention rate was 104.2%, while the original material (LiFePO₄/C) is only 79.6%. The rate performance was also greatly improved. The coated material could still reach 107.1 mAh·g^{-1} at 5C, which is 39.3% higher than the original material (LiFePO₄/C). The significant improvement in electrochemical performance was attributed to the three-dimensional conductive network formed by the composite coating layer, which increased the conductivity of the material and the migration rate of lithium ions.

1. INTRODUCTION

Due to the exhaustion of traditional energy sources and the increasing demand for energy, storage battery, as the power source of the whole EVs system, has drawn more and more attention during recent years. Among various sorts of battery materials, LiFePO4 is considered as the most promising electrode material due to its abundant raw materials, no memory effect, environment-friendly, high theoretical

capacity (170 mAh·g-1), Excellent safety performance[1,2]. However, its poor ionic conductivity and poor electrochemical performance at low temperature hinder its large-scale application to some extent[3,4].

To improve the electrochemical performance of $LiFePO_4$ as the cathode materials, especially improve the electronic conductivity and migration rate of lithium ion, various strategies have been implemented, such as particle size minimization [5,6], ion doping [7,8], carbon-coating [9,10] as well as metal nano particles deposition [11,12]. Among them, surface modification is considered as an effective way to improve the electrochemical performance of LiFePO4. LiH_2PO_4 and $Fe(CH_3COO)_2$ as raw materials and few starch as carbon source and reducing agent, Bai et al. [13] synthesized $LiFePO_4$/carbon nanowires with three-dimensional (3D) nano-network structure. After sintering, carbon source carbide changed to be carbon film coating $LiFePO_4$, not only can it improve the conductivity of the materials, but also inhibit the growth or reunion of the particles, which evidently improved the electrochemical performances of $LiFePO_4$-based lithium ion batteries; Tang et al. [14] found that the cycle and rate properties of C-LiFePO4/graphene electrode materials prepared by one-step synthesis method were greatly improved, and the performance improvement was related to the interfacial tunneling effect. Mi et al. [15] reported that the co-modification of silver and carbon did not affect the olivine structure of $LiFePO_4$, but improved its kinetics in terms of discharge capacity and rate capability. Shao et al. [16] got the $LiFePO_4$/C/Ag composite hollow nano-fibers by calcination of the coaxial electro spun nano-fibers with polyvinyl pyrrolidone (PVP) as core and $[LiOH + Fe(NO_3)_3 + H_3PO_4]$/PVP/$AgNO_3$ as shell. At the current density of 0.2 C, the initial discharge capacity of LiFePO4/C/Ag hollow nano-fibers was 138.71 mAh·g-1, which is much higher than that of LiFePO4/C nanofiber electrode, the improvement of electrochemical performance was due to the introduction of silver nanoparticles, which improved the ionic conductivity of the material. Park et al. [17] reported that the LiFePO4 cathode materials coated with approximately 1wt.% silver could also maintain a high capacity at a high current density. Therefore, some electronic conductive materials (Ag or C et al.) coating could be effective to improve electrochemical performance.

However, these previous studies involving modification have always focused on the zero-dimensional (0D) metal nanoparticles (Ag、Au、Cu et al) or carbon-coating to improve the electrochemical performance, but no one-dimensional (1D) metal material was put forward for the purpose. In order to improve the conductivity of $LiFePO_4$ cathode material, we prepared spiral Ag nanochains (Ag-NCs) instead of Ag nanoparticles as one-dimensional conductors, and formed a three-dimensional conductive network with the assistance of graphene. The purpose of improving material performance is achieved.

2. EXPERIMENTAL

2.1 Materials

$LiFePO_4$/(C + RGO)/Ag-NCs composite material was prepared by hydrothermal combined chemical deposition method. The samples were synthesized by LiOH·H_2O (Shanghai Chemicals),

H₃PO₄ (≥80%, Shanghai Chemicals), FeSO₄·7H₂O (≥99 %, Shanghai Chemicals), glucose(≥99%, Shanghai Chemicals), AgNO₃ (≥99%, Shanghai Chemicals), NH₃·H₂O (Shanghai Chemicals), CH₃CHO (Nanjing Chemicals), GO (Made Via Hummers Method) along with Ascorbic acid (≥99%, Shanghai Chemicals) as reductive agent and carbon source.
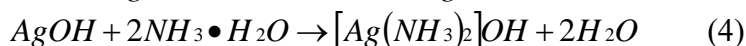
2.2 Synthesis of LiFePO₄/C+RGO

LiFePO₄/C+RGO composite was prepared via a hydrothermal route. Firstly, 3 wt.% GO suspension was mixed with 0.6 M LiOH and 0.1 M glucose aqueous solution and then 0.2 M H₃PO₄ and 0.2 M FeSO₄ aqueous solution was added dropwise to the above solution with continues stirring for 2 h(FeSO₄·7H₂O、H₃PO₄ and LiOH·H₂O with the molar ratio of 1:1:3). Subsequently, the resulting mixture was then quickly transferred into a 100 mL Teflon-lined stainless steel autoclave and heated at 200 °C for 15 h. After cooling to the room temperature, the precipitate was filtrated and washed with deionized water, then dried at 70 °C for 6 h. After then, the powder was annealed at 600 °C for 2 h under the flowing nitrogen. The samples obtained in this method are hereafter abbreviated as LiFePO₄/C+RGO. As a contrast，LiFePO₄/C was prepared via the same conditions without adding GO suspension. Reaction process is as follows：

$$3LiOH + H_3PO_4 \rightarrow Li_3PO_4 \downarrow + 3H_2O \qquad (1)$$
$$FeSO_4 + Li_3PO_4 \rightarrow LiFePO_4 + Li_2SO_4 \qquad (2)$$

The GO can be reduced to RGO under high temperature and pressure. The by-product of Li₂SO₄ is soluble in water which can be removed easily by washing.

2.3 Preparation of 1D Ag-NCs and construction of 3D conductor network

The LiFePO₄/(C+RGO)/Ag-NCs composite was synthesized by the chemical deposition process. The precursor LiFePO₄/C+RGO was the material we have got above. Dilute NH₃·H₂O was titrated into the AgNO₃ solution (0.01 mol/L) until white precipitate disappears , and then we could get a colorless transparent silver ammonia solution. Reaction is as follows:

$$AgNO_3 + NH_3 \bullet H_2O \rightarrow AgOH \downarrow + NH_4NO_3 \qquad (3)$$
$$AgOH + 2NH_3 \bullet H_2O \rightarrow [Ag(NH_3)_2]OH + 2H_2O \qquad (4)$$

Then the above colorless solution and CH₃CHO were added dropwise into the LiFePO₄/C+RGO suspension simultaneously, heated at 80 °C with continuous stirring (500 r/min) for 4 h. In this situation, Ag(NH₃)₂⁺ was reduced and then self-assembled into 1D Ag-NCs. This reaction process is shown below:

$$2Ag(NH_3)_2OH + CH_3CHO \rightarrow 2Ag \downarrow + CH_3COONH_4 + 3NH_3 \uparrow + H_2O \qquad (5)$$
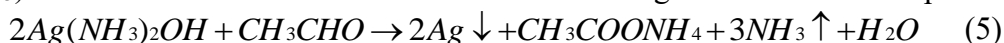
Then the 1D Ag-NCs bridged LiFePO₄/C forming a 3D conductor network with the assistance of RGO. During the reaction process, the mole ratio of AgNO₃ and NH₃·H₂O was 1:2 and we added 5% excess CH₃CHO in order for the Ag⁺ to be fully reduced. Moreover, the weight ratio of AgNO₃ and LiFePO₄/C+RGO was 1:20 to ensure that the content of Ag was 3% in the final LiFePO₄/(C+RGO)/Ag-NCs composite. After then, the solid residues were washed with distilled water and dried under vacuum at 80 °C for 12 h to collect LiFePO₄/(C+RGO)/Ag-NCs composite.

2.4 characterization and electrochemical measurements

The crystalline phase of samples were analyzed by powder X-ray diffraction (XRD, BRUKER D8) which was performed using Cu Kα radiation (λ= 1.54056 Å). Datum were collected from 10° to 80° in 2θ, with a step size of $0.05°$ at room temperature. The morphology and particle size of the prepared nanocrystals were monitored using a scanning electron microscopy (FEI SIRION200). The fine structures of prepared nanostructures were analyzed by a transmission electron microscopy (JEOL JEM-2100F).[18]

A cathode working electrode for electrochemical testing was prepared by mixing product with acetylene black as conducting agent and polyvinylidene (PVDF) as binder in N-methylpyrrolidone (NMP) with weight ratio 80:10:10.[19] Magnetic stirred until formed uniform slurry. Then the mixed slurry was spread uniformly on a thin aluminum foil and subsequently dried at 110 ^{o}C overnight under vacuum. Metal lithium foils were used as the counter electrodes. The electrolyte was 1 M LiPF6 solution in a mixed solvent of ethylene carbonate (EC) and dimethyl carbonate (DMC) (EC: DME=1:1, V/V). A polypropylene microporous film was used as the separator. The cells were assembled in an argon filled glove box. The cells were charged and discharged at room temperature between 2.0 and 4.2 V versus Li$^+$/Li on the electrochemical test instrument (CT2001A, Wuhan Land Electronic Co. Ltd., China). Cyclic voltammetry (CV) and electrochemical impendence spectroscopic (EIS) were measured by a CHI660b electrochemical workstation. CV tests were carried out at a scan rate of 0.1 mV/s in the voltage range of 2.0~4.2 V vs. Li$^+$/Li. EIS were recorded at fully discharge state of desired cycle over the frequency range of 10^5~10^{-2} Hz with the amplitude of $\pm$ 5 mV.[20,21]

3. RESULTS AND DISCUSSION
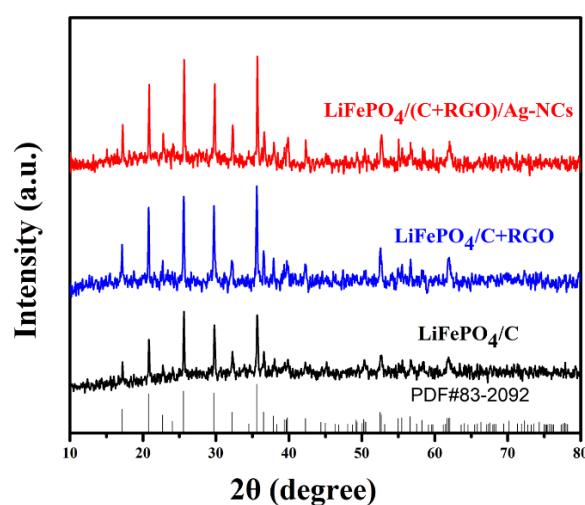
Figure 1. XRD patterns of materials

Fig.1 shows the XRD patterns of LiFePO$_4$/C, LiFePO$_4$/C+RGO and LiFePO$_4$/(C+RGO)/Ag-NCs composites. The results show that all the patterns of the samples can be readily indexed to an olivine

phase with an ordered orthorhombic crystal structure belonging to the space group Pnma, which is the same as the standard one (PDF#83-2092). The peak intensity around 38.5° for the $LiFePO_4/(C+RGO)/Ag$-NCs composite is stronger than that of the $LiFePO_4/C$ and $LiFePO_4/C+RGO$, this could prove the existence of silver (PDF#87-0720) [16]. These sharp peaks in the patterns indicate that the powders are well crystalline. The $LiFePO_4/(C+RGO)/Ag$-NCs composite contains the residual carbon and RGO, however, there is no peaks belong to carbon, it was duo to the content of coating materials is low and the residual carbon was amorphous.[22] It also indicated that the modification did not change the material crystal structure .
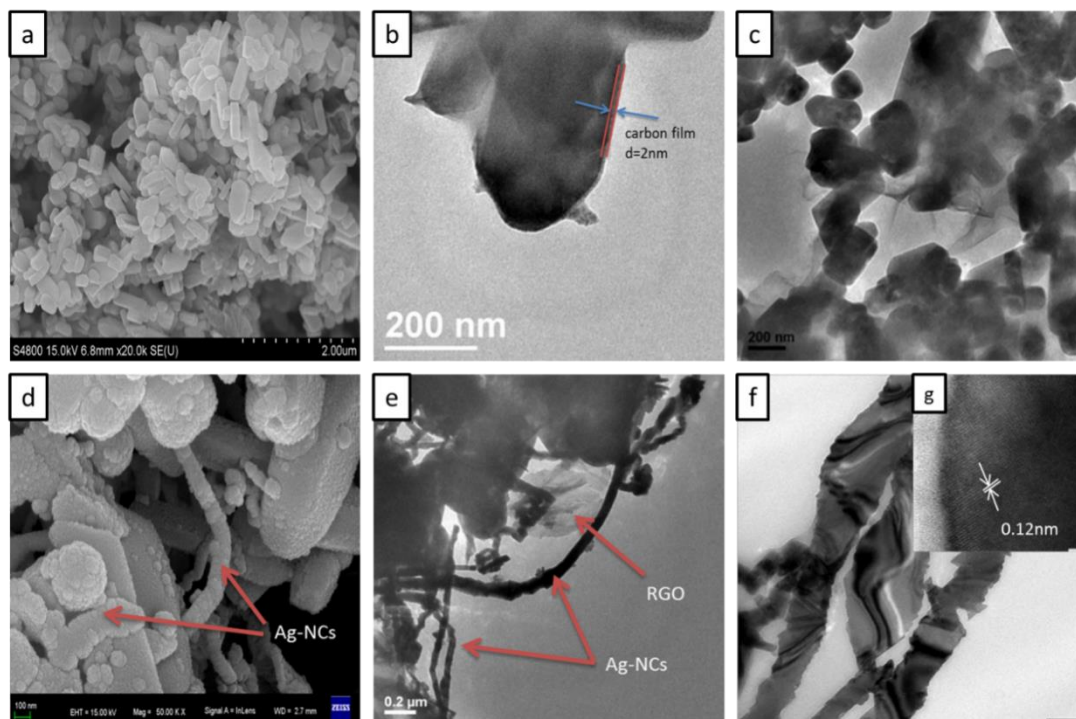

Figure 2. SEM micrograph of (a) $LiFePO_4/C$ and (d) $LiFePO4/(C+RGO)/Ag$-NCs; TEM micrograph of (b) $LiFePO_4/C$, (c) $LiFePO_4/C+RGO$, (e) $LiFePO_4/(C+RGO)/Ag$-NCs and (f) Ag-NCs;   (g) HRTEM micrograph of Ag-NCs

Fig.2 shows the micrograph of materials as-prepared. Fig.2(a) indicates that the morphology of $LiFePO_4/C$ exhibits rod-like structure with the size of 600 nm in length and 300 nm in radial direction. Fig.2(b) shows that the surface of $LiFePO_4$ was coated by carbon film which is about 2 nm, this is the result of the carbonization of glucose without oxygen under high temperature. After graphene oxide materials intervening as shown in Fig.2(c), the size of the $LiFePO_4$ are obviously optimized with the length is around 400 nm and the diameter is around 160 nm, which is smaller than the bare $LiFePO_4/C$. This is because the involvement of graphene slice layer played a similar to the role of surface active agent, reducing and inhibiting the mutual contraction and growth of materials. It can be seen from Fig.2(d),(e) and (f), the silver presented helix-like nano-chain structure with the average width of 50 nm, which has excellent electrical conductivity and well bridged the $LiFePO_4$ particles, forming the stable and complex 3D conductive network with assistence of the grapheme. The HRTEM micrograph shown

in Fig.2(g) revealed the clear lattice fringes, the spacing between the two fringes is 0.12 nm, which is in good accordance to the d spacing of (222) of Ag, this indicates that the Ag-NCs have good crystallinity. The sample with nanoscale structures could shorten the lithium ion diffusion paths and improve the transmission efficiency of lithium ion,which can enhance the electrochemical performance of cathode materials.[23]
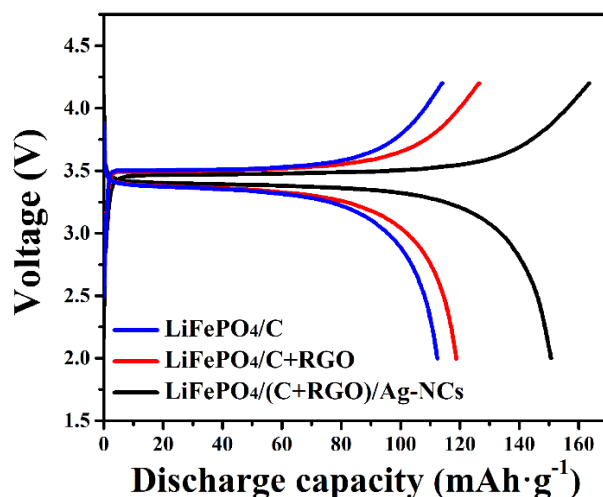
Figure 3. The initial charge and discharge curves of the $LiFePO_4/C$, $LiFePO_4/C+RGO$, $LiFePO_4/(C + RGO)/Ag-NCs$ in the potential range of 2.0-4.2V at 0.2 C
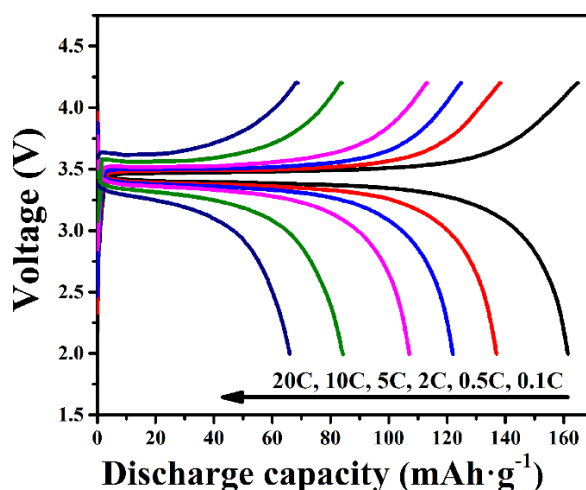

Figure 4. The charge and discharge curves of the $LiFePO_4/(C+RGO)/Ag-NCs$ in the potential range of 2.0-4.2V at different rates

The low conductivity of $LiFePO_4$ has a negative effect on the electrochemical performance, the addition of appropriate conductive agent can obviously enhance the conductivity of the material and improve the discharge capacity and other properties of the $LiFePO_4$. Fig.3 reveals the initial charge-discharge plots of the $LiFePO_4/C$, $LiFePO_4/C+RGO$ and $LiFePO_4/(C+RGO)/Ag-NCs$ electrode materials in the potential range of 2.0-4.2V versus Li^+/Li at 0.2C($36mA\cdot g^{-1}$)rate at 25°C. It shows that

all the samples exhibit typical flat charge-discharge plateaus around 3.4 V, corresponding to the Fe^{2+}/Fe^{3+} redox reaction.[24] The initial discharge capacity of $LiFePO_4/C$ is only 112.4 $mAh \cdot g^{-1}$ due to its low conductivity, however the $LiFePO_4/C+RGO$ material improves the specific capacity that reaches to 118.8 $mAh \cdot g^{-1}$ and the $LiFePO_4/(C+RGO)/Ag$-NCs that due to the introduction of silver helix-like nano-chain further improves the initial specific capacity up to 150.7 $mAh \cdot g^{-1}$[25] .Furthermore, $LiFePO_4/(C+RGO)/Ag$-NCs has stable discharge plateau, smooth discharge curve and prolonged discharge plateau which proves that the intercalation/de-intercalation of Li^+ becomes more efficient and unobstructed. It results from the introduction of RGO and Ag-NCs providing efficient electric channel, which improves the conductivity of the material.[26] Besides, the voltage difference (ΔE) of $LiFePO_4/(C+RGO)/Ag$-NCs becomes smaller between charge and discharge curves which indicates the polarizability decreases sharply. Fig.4 shows the performance of $LiFePO_4/(C+RGO)/Ag$-NCs with increasing rates from 0.1 C to 20 C between 2-4.2 V. It indicates the material has outstanding flat voltage plateaus, and the discharge voltage plateaus at different rates range from 3.5 to 3.2 V, which indicates $LiFePO_4/(C+RGO)/Ag$-NCs has an extremely stable structure[27].It also can be seen that the $LiFePO_4/(C+RGO)/Ag$-NCs exhibits excellent rate capability with the discharge capacities of 161.5 (0.1 C)、137 (0.5 C)、122 (2 C)、107.1 (5 C)、84.3 (10 C) and 66 $mAh \cdot g^{-1}$ (20 C).

Cyclic stability is an important index of $LiFePO_4$. Fig.5(a) shows the cycle performance of $LiFePO_4/C$, $LiFePO_4/C+RGO$ and $LiFePO_4/(C + RGO)/Ag$-NCs at 0.2 C rate (25 ^{o}C). It indicates that $LiFePO_4/C$ composite co-modified by RGO and Ag-NCs has the highest specific capacity (150.7 $mAh \cdot g^{-1}$) than $LiFePO_4/C$ and $LiFePO_4/C+RGO$. Interestingly, we could find clearly the specific capacity increase to 157 $mAh \cdot g^{-1}$ after 100 cycles with capacity retention of 104.2%, which shows excellent cycle performance. This phenomenon is more evident in $LiFePO_4/C+RGO$, the specific capacity increases from 120.1 $mAh \cdot g^{-1}$ to 138.7 $mAh \cdot g^{-1}$ after 100 cycles with capacity retention of 115.5% which is higher than MnOx/C-LFP composites(96.9%)[28]. However the specific capacity of $LiFePO_4/C$ decays seriously from 112.1 $mAh \cdot g^{-1}$ to 89.2 $mAh \cdot g^{-1}$ after 100 cycles, the capacity retention is only 79.6%. The cycle performance of the $LiFePO_4/(C + RGO)/Ag$-NCs have been significantly improved, perhaps it is because of the 3D conductive network formed by the 1D Ag-NCs with the assistance of 2D grapheme, which enhanced the electric conductivity and formed a clear electric mobility channel[29]. Moreover, the graphene with laminar structure acts as a storage for Li^+, more Li^+ are embedded and released in the cycle, which is the reason of specific capacity increase gradually [10]. Fig.5(b) shows the rate performances of $LiFePO_4/C$, $LiFePO_4/C+RGO$ and $LiFePO_4/(C+RGO)/Ag$-NCs at different current rate. Among them, $LiFePO_4/(C+RGO)/Ag$-NCs has the highest specific capacity and the lowest capacity loss. It is because 3D conductive network formed by Ag-NCs and RGO plays an important role as the structure stabilizers during charging and discharging process, it can restrain the structural collapse and ensure the integrity of the material structure at high current density[30]. In a word, all the results indicate $LiFePO_4/(C+RGO)/Ag$-NCs has excellent structure stability and remarkable electrochemical performance.
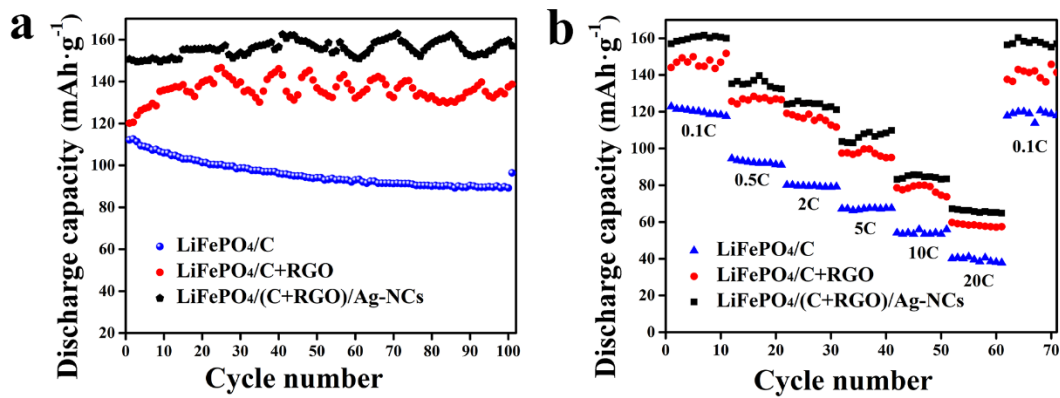
Figure 5. (a) cycle performance of LiFePO₄/C, LiFePO₄/C+RGO, LiFePO₄/(C+RGO)/Ag-NCs at 0.2 C rate, (b) cycle performance of LiFePO₄/C, LiFePO₄/C+RGO and LiFePO₄/(C+RGO)/Ag-NCs at different rates
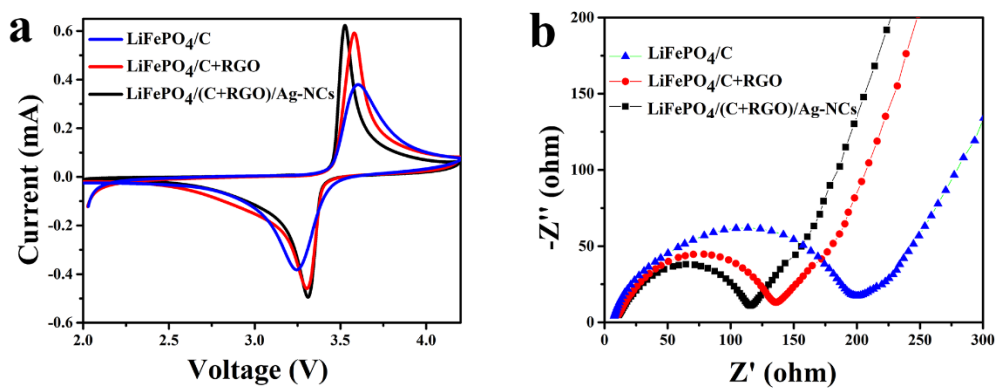
Figure 6. (a) CV , (b) EIS curves of LiFePO₄/C, LiFePO₄/C+RGO and LiFePO₄/(C+RGO)/Ag-NCs after three cycles at 0.2 C rate

To get insight into the kinetics of intercalation/de-intercalation, the cyclic voltammetry (CV) and electrochemical impedance spectroscopy (EIS) were carried out at room temperature. Fig.6(a) shows the CV curves of LiFePO₄/C, LiFePO₄/C+RGO and LiFePO₄/(C+RGO)/Ag-NCs after three cycles at 0.2 C. It can be found that the voltage difference between oxidation and reduction peaks of LiFePO₄/C+RGO (3.58/3.305 V) and LiFePO₄/(C+RGO)/Ag-NCs (3.526/3.31 V) are smaller than that of LiFePO₄/C (3.548/3.245 V), the LiFePO₄/(C+RGO)/Ag-NCs'is the smallest. The reaction peaks of materials are ascribed to the Fe^{3+}/Fe^{2+} redox couple transformation, the smaller redox potential difference means the lower electrode polarization and higher lithium ion diffusion rate. LiFePO₄/(C+RGO)/Ag-NCs also has the highest current peak intensity, indicating that the lithium ion intercalation and de-intercalation reactions are stronger. The CV test is an effective approach to value the electrochemical reaction reversibility[31]. The results imply LiFePO₄/(C+RGO)/Ag-NCs exhibits admirable reversibility and good reaction kinetics during the charge-discharge cycling. Fig.6(b) shows the EIS spectra of LiFePO₄/C, LiFePO₄/C+RGO and LiFePO₄/(C+RGO)/Ag-NCs. The overall profiles exhibit a semicircle at high frequency region and a straight line at low frequency region. The semicircle part is attributed to

the charge-transfer resistance (R_{ct}) which is responsible for the capacity attenuation of the cathode material [8]. Fig.6 (b) shows distinct decrease of R_{ct} from 199.9 Ω (LiFePO$_4$/C) to 135.9 Ω (LiFePO$_4$/C+RGO) until descend to 115.6 Ω (LiFePO$_4$/(C+RGO)/Ag-NCs), which indicates the charge transfer reaction of the LiFePO$_4$ is enhanced and the transportation of electrons is improved by the 3D conduction network formed by 1D Ag-NCs assisted with 2D RGO. The straight line at the low frequency indicates that the diffusion resistance of the Li$^+$ and the slope of the line reveals the diffusion coefficient of Li$^+$. The reduce of the particles size results in the increase of the diffusion coefficient of Li$^+$, and shortens the distance of Li$^+$ diffusion. As previous analyses showed that Ag-NCs did not get into LiFePO$_4$ crystal lattice and not change the particles size, morphology and structure, so LiFePO$_4$/C+RGO and LiFePO$_4$/(C+RGO)/Ag-NCs have the similar slope. However, the slope for LiFePO$_4$/C is larger than LiFePO$_4$/C+RGO and LiFePO$_4$/(C+RGO)/Ag-NCs due to it is larger size[32]. In conclusion, LiFePO$_4$/(C+RGO)/Ag-NCs has the lowest resistance, and its electrochemical performance should be the best,which is consistent with the previous analysis.

4. CONCLUSIONS

In summary, the well crystalline LiFePO$_4$/(C+RGO)/Ag-NCs cathode composite material for lithium ion battery was successfully prepared by hydrothermal combining with chemical deposition method. This work provided a new method for using one-dimensional metal materials as wires to construct a three-dimensional network that enhanced the conductivity of LiFePO$_4$ materials. Ag-NCs were connected to form a three-dimensional conductive network with the help of graphene, which was beneficial to improve the electrochemical performance of the prepared material. Electrochemical performance tests showed that LiFePO$_4$/(C+RGO)/Ag-NCs had good discharge capacity and good cycle performance under different current densities.The cycle performance of the coated material has been significantly improved, which may be due to the formation of a three-dimensional conductive network by 1D Ag-NCs with the assistance of 2D graphene, which made LiFePO$_4$/(C+RGO)/Ag-NCs show good cycle and rate performance. In addition, the graphene layer acted as a Li$^+$ storage layer, allowing more Li$^+$ to be inserted and extracted during the cycle, which was the reason for the gradual increase in specific capacity. Therefore, we successfully prepared a modified LiFePO$_4$ cathode material with high electrochemical performance.

References

1. A. K. Padhi, K. S. Nanjundaswamy, and J. B. Goodenough, *J. Electrochem. Soc.*, 144(1997)1188.

2. S. Y. Chung, J. T. Bloking, and Y. M. Chiang, *Nature Mater.*, 1(2002)123.
3. Y. Hou, X. Wang, Y. Zhu, C. Hu, Z. Chang, Y. Wu, and R. Holze, *J. Mater. Chem. A*, 1(2013)14713.
4. T. Zhang, X. B. Cheng, Q. Zhang, Y. Lu, and G Luo, *J. Power Sources*, 324(2016)52.
5. C. Sun, S. Rajasekhara, J. B. Goodenough, and F. Zhou, *J. Am. Chem. Soc.*, 133(2011)2132.
6. W. J. Zhang., *J. Electrochem., Soc.*, 157(2010)A1040.
7. J. Tu, K. Wu, H. Tang, H. Zhou, and S. Jiao, *J. Mater. Chem*. A, 5(2017)17021.
8. Q. Liu, W. Liu, D. Li, and Z. Wang, *Mater. Lett.*, 162(2016)87.
9. J. Lim, Y. Li, D.H. Alsem, H. So, S. C. Lee, P. Bai, D.A. Cogswell, X. Liu, N. Jin, Y.S. Yu, N. J. Salmon, D.A. Shapiro, M.Z. Bazant, T. Tyliszczak, and W. C. Chueh, *Science*, 353(2016)566.
10. Lung-Hao Hu, By, Wu, Feng-Yu, Lin, Cheng-Te, Khlobystov, Andrei N., Li, and Lain-Jong, Nature Communications, 4(2013)1687.
11. D. Shao, J. Wang, X. Dong, W. Yu, G. Liu, F. Zhang, and L. Wang*, J Mater Sci: Mater Electron*, 24(2013)4718.
12. J. Tu, X. B. Zhao, G. S. Cao, J. P. Tu, and T. J. Zhu, *Mater. Lett.*, 60(2006)3251.
13. N. Bai, K. Xiang, W. Zhou, H. Lu, X. Zhao, and H. Chen, *Electrochim. Acta*, 191(2016)23.
14. H. Tang, Y. Si, K. Chang, X. Fu, B. Li, E. Shangguan, Z. Chang, X. Z. Yuan, and H. Wang, *J. Power Sources*, 295(2015)131.
15. C. H. Mi, Y. X. Cao, X. G. Zhang, X. B. Zhao, and H. L. Li, *Powder Technol.*, 181(2008)301.
16. D. Shao, J. Wang, X. Dong, W. Yu, G. Liu, F. Zhang, and L. Wang, *J. Mater. Sci.: Mater. Electron.*, 24(2013)4718.
17. K. S. Park, J. T. Son, H. T. Chung, S. J. Kim, C. H. Lee, K. T. Kang, and H. G. Kim., *Solid State Commun.*, 129(2004)311.
18. Y. Li, H. Xu, P.H. Chien, N. Wu, S. Xin, L. Xue, K. Park, Y.Y. Hu, J.B. Goodenough, *Angew. Chem. Int. Ed.*, 57(2018)8587.
19. G. Du, Y. Zhou, X. Tian, G. Wu, Y. Xi, S. Zhao, *Appl. Surf. Sci.*, 453(2018)493.
20. D. Li, D.L. Danilov, B. Zwikirsch, M. Fichtner, Y. Yang, R.A. Eichel, P.H.L. Notten, *J. Power Sources,* 375(2018)106.
21. T. Pareek, S. Dwivedi, B. Singh, D. Kumar, P. Kumar, S. Kumar, *J. Alloys Compd.*, 777 (2019) 602.
22. Z. Wu, W. Ren, L. Xu, F. Li, H. Cheng, *ACS Nano*, 5(2011)5463.
23. B. Wang, B. Xu, T. Liu, P. Liu, C. Guo, S. Wang, Q. Wang, Z. Xiong, D. Wang,X. Zhao, *Nanoscale,* 6(2014)986.
24. Yu-Xuan Bai, Jing Zhang, Yu-Bing Yang, Rong Yang, Ying-Lin Yan, and Juan Wang, *Journal of Alloys and Compounds*, 843(2020)154915.
25. Xufeng Wang, Zhijun Feng, Xiaolong Hou, Lingling Liu, Min He, Xiaoshu He, Juntong Huang, and Zhenhai Wen, *Chemical Engineering Journal*, 379(2020)122371.
26. M. Fingerle, C. Loho, T. Ferber, H. Hahn, R. Hausbrand, *J. Power Sources*, 366(2017)72.
27. Q. Liu, Z. Geng, C. Han, Y. Fu, S. Li, Y.B. He, F. Kang, B. Li, *J. Power Sources*, 389(2018)120.
28. [Su Jin Kim, Jae-Hyun Cho, Kwan-Young Lee, Byung Won Cho, Kyung Yoon Chung, and Ji-Young Kim, *Bulletin of the Korean Chemical Society*, 40(2019)317.
29. C. Shao, H. Liu, Z. Yu, Z. Zheng, N. Sun, C. Diao, *Solid State Ionics*, 287(2016)13.
30. S. Ohta, T. Kobayashi, T. Asaoka, *J. Power Sources*, 6(2011)196.
31. K. Takada, *Acta Mater.,* 61(2013)759.